# Track reconstruction in the BESⅢ muon counter*

LIANG Yu-Tie(梁羽铁)[1;1)] LIU Kun(刘坤)[1] YOU Zheng-Yun(尤郑昀)[1] MAO Ya-Jun(冒亚军)[1;2)]
LI Wei-Dong(李卫东)[2;3)] BIAN Jian-Ming(边渐鸣)[2,3] CAO Guo-Fu(曹国富)[2,3]
CAO Xue-Xiang(曹学香)[2,3] CHEN Shen-Jian(陈申见)[4] DENG Zi-Yan(邓子艳)[2]
FU Cheng-Dong(傅成栋)[2] GAO Yuan-Ning(高原宁)[5] HAN Lei(韩磊)[6] HAN Shao-Qing(韩少卿)[7]
HE Kang-Lin(何康林)[2] HE Miao(何苗)[2] HU Ji-Feng(胡继峰)[3] HU Xiao-Wei(胡小为)[4]
HUANG Bin(黄彬)[2,3] HUANG Xing-Tao(黄性涛)[8] JIA Lu-Kui(贾卢魁)[2,3] JI Xiao-Bin(季晓斌)[2]
LI Hai-Bo(李海波)[2] LIU Bei-Jiang(刘北江)[2,3] LIU Chun-Xiu(刘春秀)[2] LIU Huai-Min(刘怀民)[2]
LIU Ying(刘颖)[9] LIU Yong(刘勇)[2,3] LUO Tao(罗涛)[2,3] LÜ Qi-Wen(吕绮雯)[10] MA Qiu-Mei(马秋梅)[2]
MA Xiang(马想)[2,3] MAO Ze-Pu(毛泽普)[2] MO Xiao-Hu(莫晓虎)[2] NING Fei-Peng(宁飞鹏)[10]
PING Rong-Gang(平荣刚)[2] QIU Jin-Fa(邱进发)[2] SONG Wen-Bo(宋文博)[11] SUN Sheng-Sen(孙胜森)[2]
SUN Xiao-Dong(孙晓东)[2,3] SUN Yong-Zhao(孙永昭)[2] TIAN Hao-Lai(田浩来)[2,3] WANG Ji-Ke(王纪科)[2,3]
WANG Liang-Liang(王亮亮)[2,3] WEN Shuo-Pin(文硕频)[2] WU Ling-Hui(伍灵慧)[2,3] WU Zhi(吴智)[2,3]
XIE Yu-Guang(谢宇广)[2] XU Min(徐敏)[12] YAN Jie(言杰)[12] YAN Liang(严亮)[2,3] YAO Jian(姚剑)[11]
YUAN Chang-Zheng(苑长征)[2] YUAN Ye(袁野)[2] ZHANG Chang-Chun(张长春)[2]
ZHANG Jian-Yong(张建勇)[2] ZHANG Lei(张雷)[4] ZHANG Xue-Yao(张学尧)[8] ZHANG Yao(张瑶)[2]
ZHENG Yang-Heng(郑阳恒)[3] ZHU Yong-Sheng(朱永生)[2] ZOU Jia-Heng(邹佳恒)[8]

1 (School of Physics and State Key Laboratory of Nuclear Physics & Technology, Peking University, Beijing 100871, China)
2 (Institute of High Energy Physics, CAS, Beijing 100049, China)
3 (Graduate University of Chinese Academy of Sciences, Beijing 100049, China)
4 (Nanjing University, Nanjing 210093, China)
5 (Tsinghua University, Beijing 100084, China)
6 (Henan Normal University, Henan 453007, China)
7 (Nanjing Normal University, Nanjing 210097, China)
8 (Shandong University, Jinan 250100, China)
9 (Guangxi University, Nanning 530004, China)
10 (Shanxi University, Taiyuan 003006, China)
11 (Zhengzhou University, Zhengzhou 450001, China)
12 (Department of Modern Physics, University of Science and Technology of China, Hefei 230026, China)

**Abstract** The reconstruction algorithm for BESⅢ Muon Counter, MucRecAlg, is developed with the object-oriented language C++ in BESⅢ offline software environment. MucRecAlg consists of the following functions:

Received 4 November 2008, Revised 21 November 2008
* Supported by National Natural Science Foundation of China (10375002, 10675004, 10821063), Research and Development Project of Important Scientific Equipment of CAS (H7292330S7)
1) E-mail: liangyt@hep.pku.edu.cn
2) E-mail: maoyj@pku.edu.cn
3) E-mail: liwd@ihep.ac.cn

to find track seeds either from extrapolation of tracks in the main drift chamber or from the fired strips in muon counter, to select fired strips associated to the candidate tracks, to fit the candidate tracks with a linear or quadratic function and to calculate other parameters of the tracks for muon identification. Monte Carlo samples are generated to check the performance of the reconstruction package, such as reconstruction efficiency, muon remaining rate and pion rejection rate, etc. The preliminary results show that the pion rejection rate is around 3%—4% while the muon remaining rate is better than 90% in 0.4—1.6 GeV/$c$ momentum region, which meets the requirement as shown in the design report.

**Key words** BESIII, MUC, reconstruction

**PACS** 24.10.Lx, 29.40.Cs, 29.40.Gx

## 1 Introduction

The Beijing Spectrometer III (BESIII[1]) is a general purpose detector, which will be running at the Beijing Electron-Positron Collider II (BEPCII), for many important tau-charm physics targets.

The BESIII consists of four sub-detectors: Main Drift Chamber (MDC), Time-Of-Flight (TOF), Electro-Magnetic Calorimeter (EMC), and Muon Counter (MUC). The MUC is a gaseous detector using Resistive Plate Chambers (RPCs). It's designed to measure the position and penetrating depth of charged particles (particularly muons), and then to identify muons from hadrons. So track reconstruction in the MUC plays an important role in BESIII offline data processing and analysis.

This paper introduces the process of the MUC reconstruction algorithm, MucRecAlg, which has been developed in the framework of BESIII Offline Software System (BOSS)[2]. Firstly, it gives a short introduction to the MUC detector, then enters into details of the track finding in MUC, such as searching for seed, attaching strips and track fitting, etc. Finally, the performance for both MUC reconstruction and particle identification is presented.

## 2 Structure of MUC

The muon detector has one barrel part and two endcaps (east endcap and west endcap). There are 9 layers in the barrel and 8 layers in each endcap. For each layer, two RPC layers and one pickup strip layer are compacted as a sandwich. The total amount of RPC units is 978, and the yielding area is up to 1272 m$^2$. Its coverage of the solid angle is about 0.83 ($\cos\theta$), and the width of the readout strip varies from 20 mm to 39 mm with 12 mm intrinsic spatial resolution for all 9152 electronics channels. The gas mixture of Argon (50%), F134a (42%) and iso-butane (8%) is chosen. The schematic view of MUC is shown in Fig. 1.

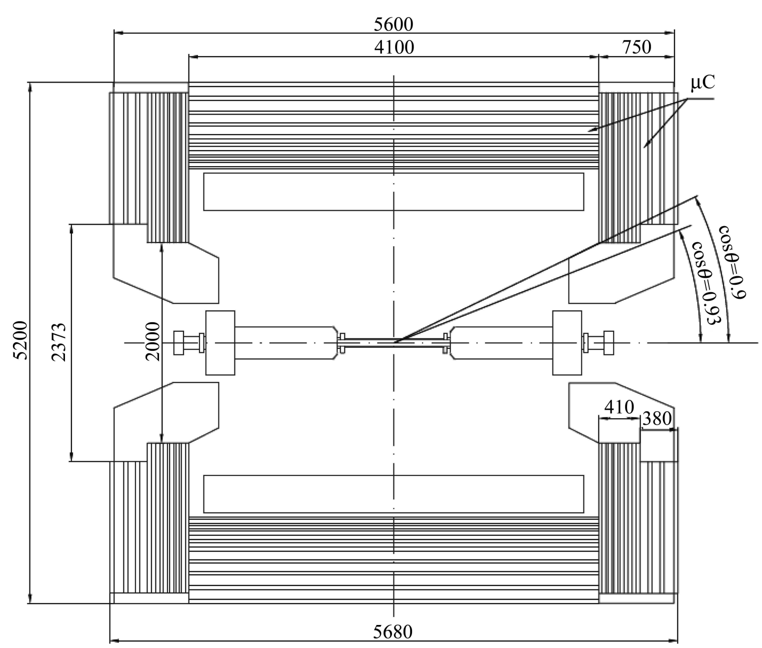


Fig. 1. A schematic view of MUC.

## 3 MUC reconstruction algorithm

Energetic particles entering the RPC will produce electrons from the gas molecules through ionization. These electrons will be accelerated by the electric field provided by high voltage source and as a result they will liberate more electrons. Enough gas molecules are eventually ionized to allow the liberated electrons to form a spark. The formed spark induces a voltage in an adjoining readout module. This voltage is then sent as a signal to the electronic end. These signals are recorded by the DAQ system and stored in raw data. The MUC reconstruction algorithm handles the raw data and reconstructs MUC tracks. The following is a detailed description of the reconstruction procedure.

The main processes of the reconstruction algorithm are to find seed, search and attach fired strips into the track, do track fitting, and calculate track parameters.

### 3.1 Track finding

TrkExtAlg[3] is an algorithm developed for extrapolating the BESIII MDC track into outer subdetectors. It considers the magnetic deflection and ionization loss of the particle in the BESIII detector. For a charged particle with high transverse momentum, the reconstruction efficiency in MDC is close to 100%. It's suitable to use MDC track as seed. Fired strips in the muon counter could also be used as seed, which is mainly used in the reconstruction of cosmic-ray events.

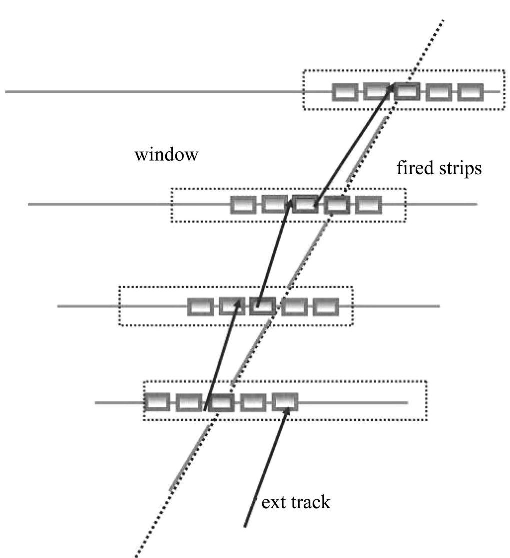


Fig. 2. Track finding in the MUC.

With the seed, track finding in MUC can start. The search from track candidates in MUC will start firstly in the barrel and then in the endcaps. Using the extrapolated track from MDC as a seed (Fig. 2), it's easy to find the interaction point and direction of this track in the first layer of MUC. Then, the algorithm calculates the distance between the interaction point and the fired strip in this layer and attaches the strip within a predefined window. Maybe more than one strip attached in a layer. With this new strip, the interaction point and direction of the track candidate will be recalculated. With the new parameters, the search for MUC track will be repeated in the next layer. The iteration procedure will be stopped when the last MUC layer is met.

The window size varies from 6 to 10 strips for different layers. We have studied the distribution of the above window size in each layer for both barrel and endcaps, and have found that the RMS value in each layer is between 30 to 50 mm. So the predefined window size (240 to 320 mm) is about 6$\sigma$ of the distance distribution. This means very few hits will be lost but maybe some noise hits included. The number of RPC noise hit for an event, $N$, is given by (1):

$$N = n \times A \times T \approx 1 \text{ (hit/event)}, \quad (1)$$

where the RPC background level ($n$) is less than 0.1 Hz/cm$^2$, the yielding area ($A$) is up to 1272 m$^2$, and the time gating ($T$) of an event is about 800 ns.

Due to the low noise level, the window size is reasonably big to include more hits in track finding.

### 3.2 Track fitting

The BESIII global coordinate ($x$, $y$, $z$) and the local coordinate ($x'$, $y'$, $z'$) for each segment of the barrel are shown in Fig. 3. In the global coordinate, the $z$ axis is parallel to the pipe, and the $y$ axis is perpendicular to the ground. In the local coordinate, the $z'$ axis is parallel to the pipe, the $y'$ axis is perpendicular to the layer of the segment. So, the local coordinate for each segment is rotated around $z$ axis with an angle. For the endcaps, the local coordinate in each segment also exists, but $x'$, $y'$, and $z'$ axes are always parallel to $x$, $y$, and $z$ axes, respectively.

The MUC strip is designed to have one dimensional readout. In barrel, strips in even layers are called $\phi$-strips because they are parallel to the $z$ axis and each one has a fixed $\phi$ value. Strips in odd layers, perpendicular to the $z$ axis, are named $z$-strips. In the endcaps, strips with fixed $x$ value in odd layers are called $x$-strips and those with fixed $y$ value in even layers are called $y$-strips.

In the phase of track finding, the hits, fired strips, lying in a track are put into a different collection according to their orientation. After track finding we have two hit collections for $\phi$-strips and $z$-strips in the barrel, and another two hit collections for $x$-strips and $y$-strips in the endcaps.

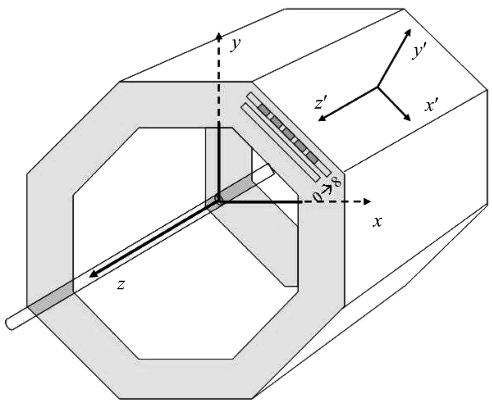


Fig. 3. Global coordinate and local coordinate systems.

Assuming the effect of magnetic field is neglectable in MUC, the path of charged particle is close to a straight line. The linear fit can be applied to $\phi$-strips in $x$-$y$ plane and to $z$-strips in the $y'$-$z'$ plane, respectively. In the endcaps, the linear fit is applied in the $y$-$z$ plane and the $x$-$z$ plane for $y$-strips and $x$-strips, respectively. There must be 2 hits in different layers for each fit.

The $\chi^2$ of the fit is defined as:

$$\chi^2 = \frac{\sum_i (d_i/w_i)^2}{N_{\rm dof}} \tag{2}$$

in which $d_i$ is the distance from the center of each strip to the interaction point of the track with this layer, $w_i$ is the width of this strip and $N_{\rm dof}$ is the number of degree of freedom of the track. If the $\chi^2$ is too big, which means track fitting is bad, this track will not be used in further studies.

In this case, we get two-dimensional straight line in each readout orientation which is in local coordinate. One three-dimensional line in BESIII coordinate is needed in the further calculation.

For the barrel, the slopes of 3D line could be calculated with the following equation.

$$v_x = \frac{v_{y'z'} \times {\rm Sign}(v_{xy})}{\cos(\delta\phi)\sqrt{(1+v_{xy}^2)}}, \tag{3}$$

$$v_y = v_{xy} \times v_x \tag{4}$$

in which $v_{y'z'}$ ($v_{xy}$) is the slope of 2D line in $x$-$y$ ($y'$-$z'$) coordinate, and $v_x$ ($v_y$) is the slope of projection of 3D line in $z$-$x$ ($z$-$y$) coordinate. $\delta\phi$ is the angle between the 2D line and $y'$ axis.

For the endcaps, the local coordinates are subsets of the BESIII coordinate. The 3D line could be derived directly with two 2D straight lines.

In fact, the magnetic field in MUC is about 1 Tesla. Estimating a muon with momentum 1 GeV/$c$, will bend about 2 strips when passing through MUC vertically with magnetic field. Considering the effect of magnetic field, we implemented the quadratic fitting method. There must be 3 layers at least in each readout dimension.

In linear fitting, a three-dimensional line is combined. The direction and initial position of this track are updated with this three-dimensional line. While quadratic fitting is used to calculate the penetrating depth and $\chi^2$ of the MUC track but not the direction or position. So, we need not combine two readout dimensions.

After the track fitting, we will calculate some reconstruction quantities, such as the penetrating depth, the maximum number of hits per layer, the match distance, etc.

## 4 Performance

The performance of MUC reconstruction has been studied with the Monte Carlo data sample. In the MC simulation, the detection efficiency for MUC strips is obtained from the cosmic-ray experiment, and noise is not added. We have produced 50000 single muon events in the momentum range from 0.4 GeV/$c$ up to 1.6 GeV/$c$ with $-0.93 < \cos\theta < 0.93$, where $\theta$ is the incident polar angle. Muons could not reach MUC when the momentum is below 0.4 GeV/$c$. We have also produced 20000 muon pair events from J/ψ decay.

### 4.1 Reconstruction efficiency

In single muon events, the reconstruction efficiency could be simply defined as the number of reconstructed tracks divided by the number of events with MUC hits. In this definition, the effect of detector acceptance has been taken into account.

The reconstruction efficiency as a function of transverse momentum is shown in Fig. 4. The efficiency reaches 99% when the transverse momentum reaches up to 0.7 GeV/$c$. To study the quality of the reconstructed track, we compared it with Monte Carlo and calculated the missing hits number. The triangular points and quadrate points in Fig. 4 are the reconstruction efficiency with 0 or 1 missing hits.

So, most of the reconstructed tracks have no missing hits.

The reconstruction efficiency in low transverse momentum is low because Mdc track extrapolation is imprecise in low transverse momentum. For pion with momentum less 0.6 GeV/$c$, the difference between the extrapolated position and MC is about 78.2 cm (0.46 rad[3]). For muon, the difference is not so big as pion, but there are still 11% muons exceeding the window size (72 cm in first layer) with transverse momentum less than 0.6 GeV/$c$.

The reconstruction efficiency for the muon track in muon pair events has also been checked. It is 99.8% consistent with the results in Fig. 4.

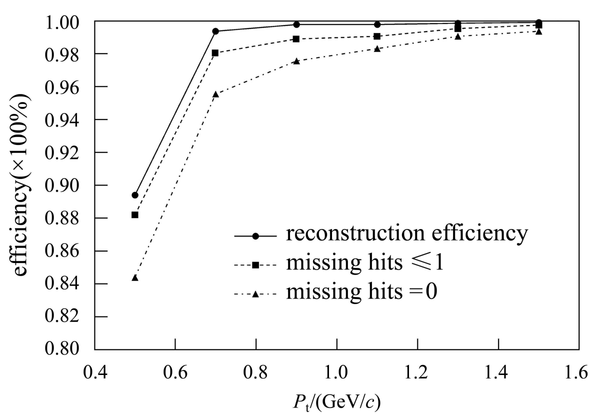


Fig. 4. Reconstruction efficiency as a function of transverse momentum for muons with and without missing hits.

### 4.2 Penetrating depth

Penetrating depth is the length of path along which particles penetrate a number of absorber layers in MUC. It is one of the most important quantities for muon identification. It can be used to distinguish muons from pions because the interaction of the muon as a lepton with material is weaker than the pion as a hadron.

We have implemented two methods to calculate the penetrating depth. One method is to accumulate the thickness of absorbers in a track, then project it to the direction of the track. The other is to find the intersection points of the track with two surfaces of absorber, then calculate the distance between them. The first implementation is fast, but can only be applied to linear trajectory when the bending power of the magnetic field is neglectable. The second method is suitable for both straight line and parabola trajectory.

After obtaining the penetrating depth from reconstruction, we compare it with the MC truth information to check our program. In the simulation, the Geant4 kernel divides the simulation process into many steps. For each step, we could retrieve all information about particles in the detector, among which the length of each step is one of them. It's easy to accumulate the step length which is much smaller than the size of the absorber in MUC. So, we could get the expected penetrating depth from Monte Carlo. Fig. 5 shows the comparison between the reconstructed depth and the expected depth. We can see from Fig. 5 that the reconstructed depth (dash line) is very close to the expected depth (solid line), which proves that the algorithm for calculation of penetrating depth works well.

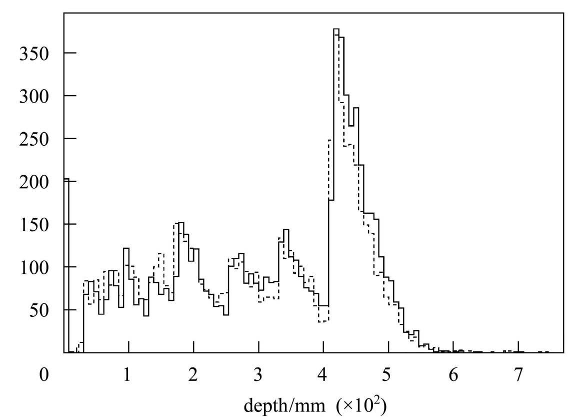


Fig. 5. Comparison of penetrating depth between simulation and reconstruction.

When the effect of magnetic field in MUC is considered, we compare the depth from linear fit with the one from quadratic fit. The mean value of difference between depth from linear fit and quadratic fit with the expected depth is 0.335 cm and 0.297 cm. The RMS value is 1.14 cm and 1.09 cm, respectively. So, the depth from quadratic fit is closer to the expected depth than that from the linear fitting. But, the difference between linear fit and quadratic fit is very small. So the penetrating depth calculated with the linear fit results is used for the performance study in this paper.

### 4.3 Direction and position

When one MUC track is initialized with a seed, the direction and position are set to be those of the extrapolated track in the first layer of MUC. After the MUC track is reconstructed, if a 3D line is formed, the direction and position of this 3D line in the first layer of MUC could be calculated. So two sets of direction and position are obtained, one from the MUC track and the other from the extrapolated track. We compare these two sets of direction and position with

MC in order to decide which one is to be used in further calculation.

In Monte Carlo simulation, we recorded the direction and position about a particle when it passed through the first RPC gas chamber. After reconstruction, we calculated the angle between MUC track (extrapolated track) and Monte Carlo, the distance between the position of MUC track (extrapolated track) and Monte Carlo. Fig. 6 shows the angle versus the distance between MUC track and MC. For most events, the distance is less than 30 mm and the angle less than 10°.

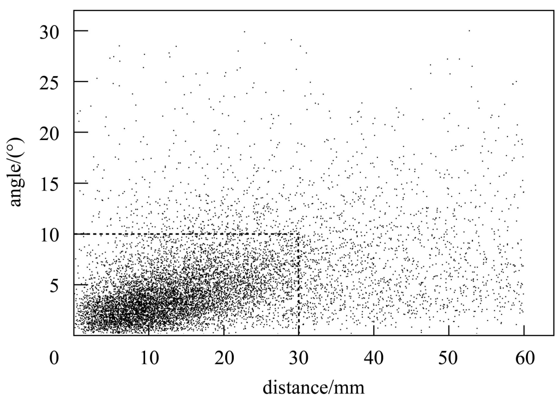


Fig. 6. Comparison of direction and position of MUC track with MC.

The mean value of the distance between MUC track and MC is about 33.4 mm, while the value from the extrapolated track is about 65.1 mm. The mean value of the angle between MUC track and MC is about 6.0°, and the value from the extrapolated track and MC is about 6.1°. There is no big difference in the direction between MUC track and extrapolated track. But the position of MUC track is obviously better than that of the extrapolated track. So, when a 3D line is constructed, the position and direction of MUC track are reserved instead of the initial values.

## 5 Muon identification

The main goal for the BESIII muon counter is to effectively separate muons from hadrons, namely to reject hadrons as many as possible while keeping muons with high efficiency. This could be achieved by measuring the specific hit pattern produced by a muon or a pion when they pass through BESIII muon counter. In principle, a muon could go deeper in the muon counter and trigger less hits in detecting layers. In contrast, a pion, for its strong interaction with absorbers, goes shallow if the interaction occur. The key to separate muons from pions is to find suit variables related to the shape of hit cluster.

In recent years, many particle identification (PID) algorithms have been developed, such as the likelihood method[4], the Fisher discriminator[5], the ***H***-Matrix estimator[6], the Artificial Neural Network[7], the Boosted Decision Tree[8], and so on.

An artificial neural network is a computational structure inspired by the study of biological neural processing. We do muon identification with the Artificial Neural Networks (ANN) method using the following reconstruction variables: penetrating depth, maximum number of hits per layer, match distance, delta phi, and momentum from drift chamber.

The maximum number of hits per layer is defined as the maximum number of fired strips in a layer for a track. This is an effective quantity to separate muons from hadrons. The muon has quite a strong punching ability, and usually it will produce only one hit in each layer. However, the hadron may produce more hits in a certain layer if a hadronic interaction occurs.

The match distance is defined as the distance between the position of muon hit and the extrapolated position by the inner track. This variable will be helpful to reduce the hadron contamination to a lower level because the hits generated by the secondary muon from the decay of pion/kaon cannot match with the inner track very well.

With MC data, we find the distribution of match distance for pion is wider than that of muon.

In magnetic field, muon and pion will bend the same angle if they have the same momentum. But considering the interaction of particles with material, the angle will be different for different particles. So, delta phi, which is the difference of phi between MUC track and MDC track, can be one of ANN variables.

In this paper, a C++ class of MultiLayer Perceptrons (MLP) in ROOT[9] library is re-used. We produce 50000 single muons and pions with momentum

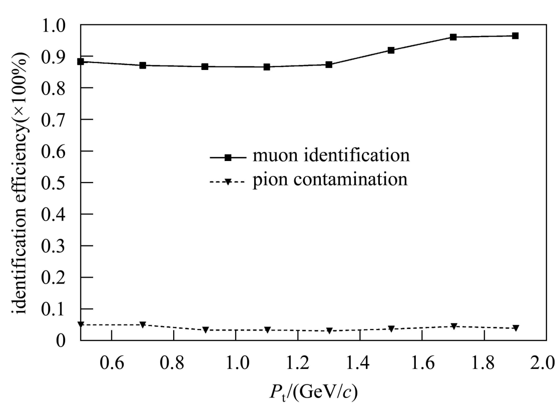


Fig. 7. Efficiency of muon identified as muon and ratio of pion misidentified as muon.

ranging from 0.4 GeV/$c$ to 1.6 GeV/$c$ and $-0.93 < \cos\theta < 0.93$, where $\theta$ is the incident polar angle. The data sample is subjected to network, and the output values are constrained to be 0,1 for pion and muon, respectively. Fig. 7 is the result of identification. We could suppress pion contamination to 4% and keep muon identification efficiency to about 90%.

Efficiency of muon identification is the ratio of the number of muons which have been identified as muon to the number of total muons. The ratio of pion contamination is the ratio of the number of pions which have been misidentified as muons to the number of total pions.

## 6 Conclusion

The reconstruction software package for BESIII MUC has been developed. Reconstruction parameters are close to Monte Carlo truth, which means that the algorithm works well. The performances are studied and basically agree well with the expected specifications in the design report.

## References

1 Preliminary Design Report of the BESIII Detector, Jan, 2004

2 LI Wei-Dong, LIU Huai-Min et al. The Offline Software for the BESIII Experiment. February 2006, Mumbai, India

3 WANG Liang-Liang et al. HEP & NP, 2007, **31**(2): 183—188 (in Chinese)

4 Carli T, Koblitz B. Nucl. Instrum. Methods A, 2003, **501**: 576—588; Holmström L, Sain R, Miettinen H E. Comput. Phys. Commun., 1995, **88**: 195

5 Fisher R A. The Use of Multijple Measurements in Taxonomic Problems. Annals of Eugenics 7, 1936, 179—188

6 Bhat P C (DØCollaboration). arXiv:hep-ex/9507007, 1995

7 Bishop C M. Neural Networks for Pattern Recognition. Oxford: Clarendon, 1998; Beale R, Jackson T. Neural Computing: An Introduction. New York: Adam hilger, 1991

8 Roe B P, YANG H J et al. Nucl. Instrum. Methods A, 2005, **543**: 577—584

9 Brun R, Rademakers F et al. An Object-Oriented Data Analysis Framework. arXiv:http://root.cern.ch